



Technical University of Crete

Department of Electrical & Computer Engineering

**Study & Design of Floating Photovoltaic Devices with  
Emphasis on Installations in the Marine Environment.**

By

Dionysios Piskopos

A thesis submitted in partial fulfillment of the requirements for the Diploma of  
Electrical and Computer Engineering.

**Thesis Committee**

Professor Stavrakakis Georgios (Supervisor)

Associate Professor Kanellos Fotios

Professor Konstantinos Belimbasakis (School of Naval Architecture & Marine Eng. NTUA)

June 9, 2021

## Περίληψη.

---

Στην σημερινή εποχή, η κλιματική αλλαγή και η πολιτική της πράσινης ανάπτυξης, καθιστούν αναγκαίο εργαλείο τις Ανανεώσιμες Πηγές Ενέργειας (Α.Π.Ε.), για την αντιμετώπιση της περιβαλλοντικής κρίσης και την μείωση των εκπεμπόμενων ρύπων. Μια από τις πιο υποσχόμενες βιομηχανίες του κλάδου των Α.Π.Ε. είναι η παραγωγή ηλιακής ενέργειας από Φωτοβολταϊκά Συστήματα (εν συντομία Φ/Β), όπου μια μεγάλη προσπάθεια είναι εν εξέλιξη με σκοπό την αύξηση της απόδοσης των Φ/Β, με ταυτόχρονη μείωση του συνολικού τους κόστους. Οι καθιερωμένες χερσαίες Φ/Β εγκαταστάσεις, ωστόσο, υποφέρουν ακόμα από σημαντικά προβλήματα όσον αφορά την αποδοτικότητα, την συντήρηση και την ενεργειακή χωριτικότητα τους, που διεκδικούνται, ανάλογα το μέγεθος εγκατάστασης και ισχύος τους.

Σε αυτή την διπλωματική, προτείνεται μια ανερχόμενη μέθοδος εγκατάστασης Πλευόμενων Φ/Β συστημάτων σε Παράκτια & Θαλάσσια Περιβάλλοντα, ( Παράκτια Πλευόμενα Φ/Β & Θαλάσσια Πλευόμενα Φ/Β), όπου αναλύονται τα βασικά ηλεκτρομηχανολογικά χαρακτηριστικά τους, τα πλεονεκτήματα & μειονεκτηματά τους σε σχέση με τα Χερσαία Φ/Β Συστήματα, και οι απόδοσή τους, μέσω δημιουργίας μοντέλων σε MATLAB με την χρήση πραγματικών ηλιακών & κλιματικών δεδομένων από τα εργαλεία PVGIS, PVSyst & Sandia PV\_LIB toolbox. Έπειτα, εξάγονται ενδιαφέροντα συμπεράσματα σχετικά με την απόδοση της συγκεκριμένης τεχνολογίας Φ/Β, ενώ σχολιάζονται η βιωσιμότητά της στην σημερινή & μελλοντική παγκόσμια & Ελληνική αγορά Ανανεώσιμων Πηγών Ενέργειας.

## **Abstract.**

---

Nowadays, climate change and «green» policies implemented all around the globe, constitute Renewable Energy Sources a necessary tool to tackle environmental crisis and diminish carbon dioxide emissions. One of the most prominent & rapidly expanding RES industries are Solar Photovoltaic Panels, or abbreviated PV, where an enormous effort is conducted to improve the efficiency of the current PV systems, while diminishing their overall cost. The well-established, Land-Based PV topologies however, occur considerable drawbacks regarding efficiency, maintenance and energy capacity, from low kWp installations, to MWp installations where the problems become more complicated and costly.

In this study, the upcoming installation alternatives of Floating Photovoltaics at Fluid and Marine environments (Inshore FPV & Offshore FPV) are discussed regarding their basic electromechanical properties, their advantages & disadvantages compared with LBPV installations, and their performance differences via MATLAB simulation models, while using solar, climate and equipment data from PVGIS, PVSyst & Sandia PV\_LIB toolbox library. Finally, simulation results are analyzed and discussed, with significant conclusions on the efficiency, viability and cost-effectiveness on the current & future global & Greek RES Market.

### *Acknowledgements.*

I would like to express my gratitude to all those involved in the construction, writing and completion of this Thesis, a task impossible to be done without their help. Special thanks to my Supervisor Professor, George Stavrakakis, for its crucial contribution in the easiest as the hardest parts of my thesis, and to my beloved father and colleague, who provided me with significant experience in the field of photovoltaics, construction techniques and the adequacy of my reporting during all these months. Finally, I would like to express my gratitude to my friends and beloved ones, who help me with various tasks and knowledge throughout my entire student career.

## Contents

---

<b>Περίληψη</b> .....	<b>1</b>
<b>Abstract</b> .....	<b>2</b>
<b>Contents</b> .....	<b>4</b>
<b>1.Introduction</b> .....	<b>1</b>
1.1 Photovoltaic System's Contribution to Tackle Environmental Crisis. ....	1
1.2 Photovoltaic Installations at Inshore and Marine Environments.....	2
1.3 PV Systems on Fluid Environments, Advantages. ....	4
1.4 PV Systems on Fluid Environments, Disadvantages.....	5
<b>2. Floating PV Systems, Electrical and Mechanical Properties</b> .....	<b>7</b>
2.1 Introduction.....	7
2.2 Inshore & Offshore FPV Construction Topologies.....	7
2.3 Integrating Photovoltaic Panels with the Water Body.....	12
2.4 Compatible Cables and Support Equipment. ....	17
2.5 Switchgear & Protection Devices.....	18
2.5.1 Fuse Disconnectors. ....	18
2.5.2 Bypass Diodes.....	19
2.5.3 Surge Protection Devices.....	19
2.5.4 Surge Protection Devices.....	19
2.5.5 Insulation Monitor Devices. ....	20
2.5.6 Residual Current Devices. ....	20
2.5.7 Main AC Circuit Breakers. ....	21
2.5.8 Main AC Load Switch.....	21
2.6 Inverters for FPV installations.....	23

2.6.1 String Inverters.....	23
2.6.1 Central Inverters.....	23
2.6.1 MMPT Power Optimizers.....	24
2.7 Grounding Methods for FPV Parks.....	24
<b>3. Simulation of Performance Differences Between FPV &amp; LBPV Parks In Crete, Greece..</b>	<b>29</b>
3.1 Introduction.....	29
3.2 Selection of Case Study Sites.....	29
3.2.1 Offshore FPV. Souda Bay, Chania, Crete .....	30
3.2.2 Inshore FPV. Souda Bay, Chania, Crete .....	31
3.2.3 Land-Based PV, Nerokouros, Chania, Crete.....	32
3.3 Significant Parameters Distinguishing FPV from LBPV Installations.....	33
3.4 Selection of Simulation Tools.....	37
3.5 Meteorological Data.....	38
3.6 Simulation Process & Results.....	39
3.6.1 Definition of the PV systems.....	39
3.6.2 Definition of Coordinates & Surrounding Characteristics.....	40
3.6.3 Integration of Irradiance and Climate Data.....	41
3.6.4 Calculation of Module Temperature.....	44
3.6.5 Calculation of Module's I/V Performance.....	45
3.6.6 Calculation of DC-AC Conversion & Overall PV Performance.....	46
<b>4. Epilogue, Conclusions &amp; Future Trends.....</b>	<b>50</b>
<b>References.....</b>	<b>52</b>
<b>Table of Figures.....</b>	<b>54</b>

# 1.Introduction

---

## 1.1 Photovoltaic System's Contribution to Tackle Environmental Crisis.

Environmental crisis due to human intervention in the ecosystems and the excessive burning of fossil fuels, is a phenomenon which bothers each and every one of us nowadays. A phenomenon responsible for the significant increase of environmental disasters, the destruction of many ecosystems and hence the instability in our climate. To tackle the consequences of this manifold problem, a global effort to enforce sustainable ways of energy production is conducted the last 20 years. Renewable Energy Sources, such as Wind Turbine Farms, Biomass Energy Production and Solar Photovoltaic Plants are one of the major contributors in this battle. Especially Solar Photovoltaic Panels or “PVs”, constitute inarguably one of the most prominent technologies in the field of Renewable Sources. In 2018, the estimated energy generation capacity of the worldwide SPVs systems was 600 TWh, 2,4% of the global energy contributed by electrical sources, value which is expected to rise exponentially up to 70% in the following decades. [1]

PV technology provides an easy, fast and low-cost solution in aspect of installation, produced energy and maintenance, compared with other alternatives such as Wind Turbines. Throughout the last decade, large scale land-based PV systems (LBPV) have been developed all around the globe (for example, Bhadla Solar Park, India – 2.25GW & Huanghe Hydropower Hainan Solar Park, China – 2.2GW [2] )with primary incentive bigger utilization of solar energy to the global electrical distribution. However, significant drawbacks have been occurred in aspect of the functionality on those projects, with most noticeable:

- High cost and low availability of land.
- Significant degradation in efficiency and life expectancy of solar panels, due to high temperatures from harsh environmental conditions, especially in heavily condensed parks.
- Concerning environmental impact in the existing ecosystems.

Based on the above, a strong motivation is emerging for alternative PV installation technologies, which combine high efficiency, low installation cost and large energy density. Floating Photovoltaic Systems are being developed the last decade, providing numerous advantages, which makes them a feasible and viable solution to more green and efficient production of solar energy. In this report, an extensive analysis is conducted to describe the properties and capabilities of Floating Photovoltaic Plants (FPV Plants) in aspect of efficiency, installation, environmental impact and more, by contrasting this technique with the classic Land Based PV installations.

## **1.2 Photovoltaic Installations at Inshore and Marine Environments.**

To understand the potential of this technology, we need to define where these floating photovoltaic parks, of FPV, are going to be installed. In term of Geography, Fluid and Marine environments include freshwater surfaces, such as natural lakes, artificial hydroelectric basins and water dam reservoirs, while the term marine environments are mainly referred to saltwater surfaces, such as at sea, in a gulf or an ocean. According to researchers in availability of freshwater surfaces globally [3], it is estimated that there are 4.550.906 km<sup>2</sup> of potentially installable FPV power, so if only 1% of those is used, it could produce 6069 TWh yearly, which covers the 25% of the worldwide electrical energy production for the year of 2015 (Total of 24215 TWh) [4].

	Surface <i>km<sup>2</sup></i>	PVPP ( $\alpha_{sw}=1\%$ ) <i>GWp</i>	PVEP <i>TWh</i>
Tropical zone	1,254,831	1,526	1,851
Temperate zone	1,506,256	1,832	2,064
Cold zone	1,789,819	2,176	2,155
Total	4,550,906	5,534	6,069

Figure 1: Potential of FPV installations, from different climate zones, (assume land usage=1%). [3]

In case of seawater surfaces availability, it's obvious that there is an abundance of the places which can be selected to install FPV plants. However, it's also obvious that in the open sea, many technical challenges are rising in aspect of structural reliability and electrical energy transportation. This is why most of the projects implemented in seawater surfaces are located in gulfs, and especially in enclosed coastline places (small gulfs), where the seawater waves are naturally or artificially limited. Although basic problems in the field of seawater applications have been occurred, such as corrosion and wave impacts, there are reliable projects of FPV in functionality for at least 5 years, such as this project in Maltese sea [5].

In both cases, those types of surfaces offer the capability for huge amounts of open surfaces with limited barricades, avoiding the significant costs for land usage and management. FPV alternatives, in general, service a specific purpose in order to expand even more the usage of Renewable Energy Sources in places where large amounts of land are not available, while providing an energy dense and compact solution.

### **1.3 PV Systems on Fluid Environments, Advantages.**

Even though FPV plant's opportunities have not been fully explored, many existing projects for up to a decade suggest many advantages for these types of Photovoltaic Parks. Below are presented some of the most noticeable advantages:

1. FPV installations require no land, except for a small amount, for usage of electrical control and protection cabinets. They provide an easy solution to avoid competing for agricultural and green zones while protecting their characteristics, their flora and fauna, while being cheaper in construction and maintenance from a similar land-based.

2. Bigger geographic potential compared to Land-Based PVs. Recent studies have concluded that FPV parks have a coefficient of 1 MWp/ha, contrary to land-based, where newer technologies in construction and efficiency have given an average of 0.5 MWp/ha to 0.7 MWp/ha [6]. In other words, we can safely conclude that we need 2/3 or even half of the Land-Based-PV area, to produce the same amount of energy.

3. Compactness in installation, easy decommissioning. Floating PV structures are based on mooring or floating mechanisms, giving the advantage of being carried out in a fully reversible way, in contrast with the land-based plants, which are fully fixed-to-the-ground structures [4]. Taking advantage of FPV's flexibility, we can easily integrate tracking techniques, as it is described later in this report.

4. Cheap cooling and tracking mechanisms. The integration of cooling techniques constitutes, relatively to land PVs, an easy and low-cost investment, excessively reduces the thermal drift effect and therefore rises the total amount of energy produced, due to the lower amounts of loses. Researches In installations of Submerged Floating Plants in Lakes & Basins, have shown an annual increase of energy production about 10% contrary to Land Based Installations [7]. Adding a Tracking System in the previous case in also easier in the most installations base on projects implemented in Singapore and Taiwan [4]. Actually, in many

cases of FPV installations, the implementations of simple and cheap tracking mechanisms further increase the produced energy of the panels up to 25%, according to case studies [4].

5. Save water while increasing its quality. One of the most demanding challenges at water saving or irrigation structures, is the ability to cover the basins/reservoirs in order to protect the water body from evaporating or, even worse, to develop big amounts of algae and many more harmful microorganisms [7]. The partial cover of this basins with FPVs, provides a cost-effective solution, while servicing the purposes mentioned previously.

6. Integration in Energy Storage Systems. The high energy and efficiency potential of an FPV integration to Hydroelectric Dams and Compressed Air Energy System Storages, providing this classic storage systems with even better stability and flexibility, reducing the effects of intermittency by the vast contribution of Renewable Energy Sources in a typical grid. The floating PV solution finds a perfect fit for the aforementioned circumstances, results which are confirmed from the majority of existed and upcoming projects in the FPV field [8].

7. Contributing on stability and independence for far offshore areas. Even though there are still many technical challenges in the field of offshore photovoltaics, the last decade offshore FPVs have been developed to provide crucial electrical support for oil-platforms, remote islands and other similar needs [9].

#### **1.4 PV Systems on Fluid Environments, Disadvantages.**

Based on the many projects implemented in FPV categories, we can distinguish the most notable difficulties that can occur to the accomplishment of this kind of projects:

1. High-cost materials and specialized equipment. Even though we mentioned that the total cost of a FPV park is cheaper than a land-based of the same power, the special environmental conditions demand high endurance constructions and anti-corrosive

materials, from the mechanical to the electrical part, increasing the overall cost of installation and commissioning. Furthermore, it is significant to note that the study and implementation for such structures requires experienced personnel and specialized study, due to incomplete standards, regulations and protocols for FPV structures in most countries.

2. Complex maintenance, less accessibility. Similar to installation, FPV parks require different and complex needs of maintenance from Land-Based PVs, due to the humidity and corrosion effects on the panels, the mooring base and the electrical equipment. These challenges are even bigger for offshore FPVs, where the distance from the nearest coastline reduces the accessibility for tactic maintenance, combined with frequent severe weather conditions (high rates of winds & waves).

3. Layout limitations, to avoid destruction from extreme conditions. In various reports about FPV projects, both at inshore and offshore applications, a significant limitation in the total installed area comes from the gap of the adjacent panels, which avert the collision of the modules, in cases of wave impacts [8]. Intuitively, the higher the wave amplitude & frequency, the longer the gap needs to be so as to avoid damages in the FPV structures. This challenge requires further area of installation per KW, and many times bigger in comparison with LBPV installations.

4. Electrical design and installation challenges. Even though there is adequate knowledge about electrical installations in fluid environments, such as ships & marines, a basic difference of an FPV installation is the permanent connection between the panels and the nearest shore, where its main electrical control equipment is located. Hence, to deal with cases of electrical faults, a strict grounding or electrical isolation system has to be designed, to ensure the safety of the near humans, wildlife & infrastructure. In the following chapters, we will explain the main methods of electrical protection to ensure the safety of the FPV park in cases of current faults.

## **2. Floating PV Systems, Electrical and Mechanical Properties.**

---

### **2.1 Introduction**

In the second Chapter of this report, we analyze the key components of an FPV structure, which is consisted of: (1) the raft-pontoon structure, (2) the solar panels and (3) the electrical systems and topologies. Recent and implemented FPV topologies are going to be described for each field with their pros and cons, accompanied with implemented results. The general purpose of the current chapter is to introduce the reader in the available solutions for constructing and commissioning FPV at inshore and offshore environments.

### **2.2 Inshore & Offshore FPV Construction Topologies.**

In aspect of buoyant constructions, various structures and bases have been designed to suit the offshore and inshore conditions, with emphasis on humidity and corrosion endurance, as well as low cost and commissioning flexibility.

A recent approach on FPV construction at water reservoirs in Singapore [8], uses tailor-made HDPE modules as a pontoon base for the Panels while creating spaces/walkways for the Inverters, cabling and maintenance. The modules are stationed in specially designed HDPE parts, indicatively see fig. 2. The HDPE modules are one-mould constructed, lightweight, high-endurance and from cheap materials, thus constitute the investment cost-effective and adequate for further expansions and advancements, such as the rotation of the whole structure to create a Tracking- similar PV topology. In general, HDPE or High-Density Polyethylene materials are very eligible and cheap for buoyant structures in inshore and offshore conditions, thus they are widely used in the FPV sector. In similar fashion, solutions with fully PVC materials with specific shapes are developed in the last 10 years, however

many challenges are occurred in the structural stiffness of the structure as well as in maintenance and accessibility. In fig. 3, a modular mono-panel module is shown, courtesy of the Ciel & Terre Company, solution widely commercialized and used in recent FPV plants.



*Figure 2: HPDE modules for Photov. Panels support at 500kW FPV Plant in Singapore.*

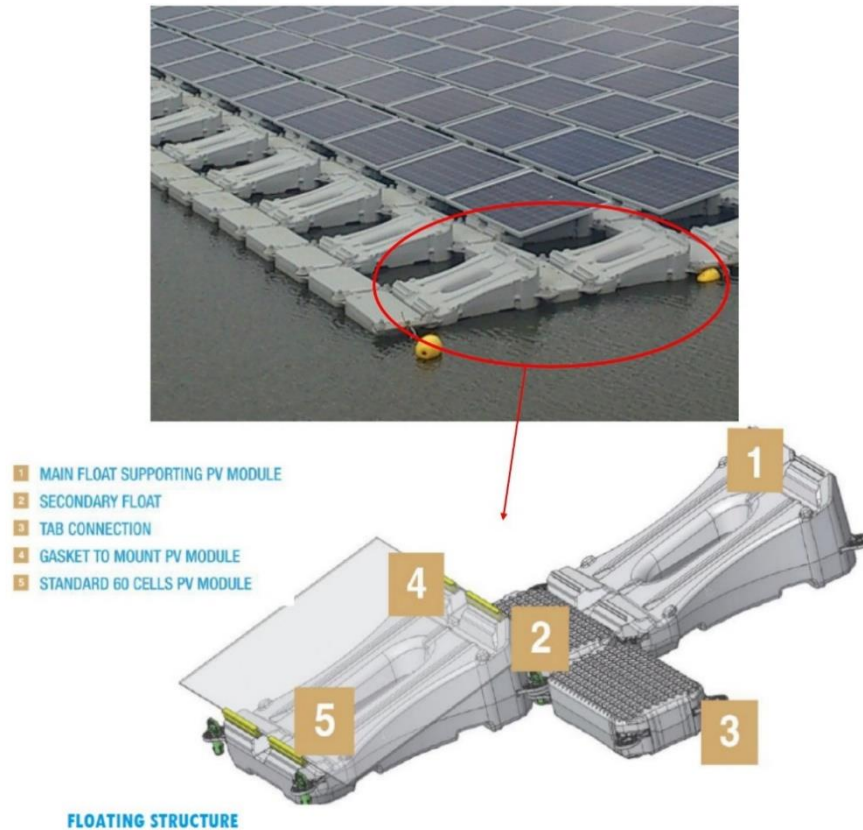


Figure 3: Specific standing panel base made of PVC, courtesy of Ciel & Terre.

Another example of inshore FPV with emphasis on HDPE components is the Terra Moretti and the Korean plant of Chengiou [10] [4], where HDPE rafts with galvanized steel were used to integrate the low corrosion with stiffness and reflection. In this case, metallic walkways are used, while the rafts are distributed in specific distances, supporting 3-6 modules each. Contrary to the above example, the panels are supported on a galvanized steel mounting bases, providing the opportunity to add reflectors and further rise the produced solar energy from the panels. The Terra Morreti and Chengiou plants are shown in *fig. 4*. Another significant advantage of the abovementioned topologies, is the avoidance of fault currents, or galvanic currents to the water body, as well as the decrease in corrosion, mainly because there is no contact between the metallic parts of the pontoon and the water body. The same property applies for the cables of the platform, which are not in contact with the

water or with the basin, due to the special gaps provided by the HDPE with classic example to be the Huainan Floating Plant in Easter Plant in fig. 5.



*Figure 4: Terra Moretti & Chengiou FPV plant.*



*Figure 5: Cabling Routing in Huainan FPV Plant, Eastern China.*

In offshore FPV topologies, a slightly different approach is used to diminish the problems of corrosion, as well as to rise the endurance and flexibility in extreme weather conditions. Very recently, one of the biggest solar energy companies in Singapore, Sunseap, constructed an offshore, 5 MWp floating solar park, with buoyant bases for the panels and for the electrical substation as well [10]. However, the panels were supported on structures made of stainless steel, protecting them from sea water corrosion. Similar to the inshore examples, many offshore projects, mostly on constructed on coastlines, have used

specialized HDPE modules like the Ciel & Terre's patent, to avoid any metallic part in the FPV structure.

Recently, a 191 KWp project of offshore FPV was installed in South Ari Atoll, Maldives, by the Austrian Company Swimsol [11]. The FPV consists of 12 independent, 60 panels platform, supported by a structure consisted of a HDPE raft, connected with stainless aluminum frames in triangular arrangement, to support the platform in cases of extreme weather conditions. Each platform is anchored on 4 drilled pointed in the 2-3m sea bottom. Classic PV panels of 265 Wp were used in 10 degrees tilt. According to Swimsol, the SolarSea type of FPV (courtesy of Swimsol), provides stiffness and flexibility, while the cabling is routed with IP67 waterproof connectors and heavy-duty pipes to the electrical station in the Coast. The FPV platforms are located approx. 30 to 50 meters from the coast. The project went on commission in mid-2019, and it was one of the biggest FPV farms in the world. Lastly, Swimsol claims that the efficiency of the FPV is increased about 10% to the land-based counterparts.



*Figure 6: Swimsol 191kW coastal FPV Plant, South Ari Atoll, Maldives.*

### **2.3 Integrating Photovoltaic Panels with the Water Body.**

To begin with, we need to remind the general types of photovoltaic panel technologies currently used in the market. An easy classification can be done by the atom bonding methods which create a polycrystalline type of panel. The most classic comparison is done by the efficiency of the panel technologies. In fig. 7, the most classic types of photovoltaic panels are compared, based on their efficiency through the 2 decades of 1993-2016 [12]. Even though we can notice efficiencies up to 45% to 50% for Multijunction Solar Panels, their market share isn't analogically high, due to very high costs of construction and industrialization. The most dominant technologies nowadays are inarguably the Multi Crystalline and Mono Crystalline Silicon Solar Panels, where their efficiency is quite moderate over the years, in the state of 15-25%. Specifically, the Multi-Si PV technologies have by far the biggest market share, due to low cost of construction and industrialization, while the Mono-Si PV is more efficient but also more expensive by the previous counterpart.

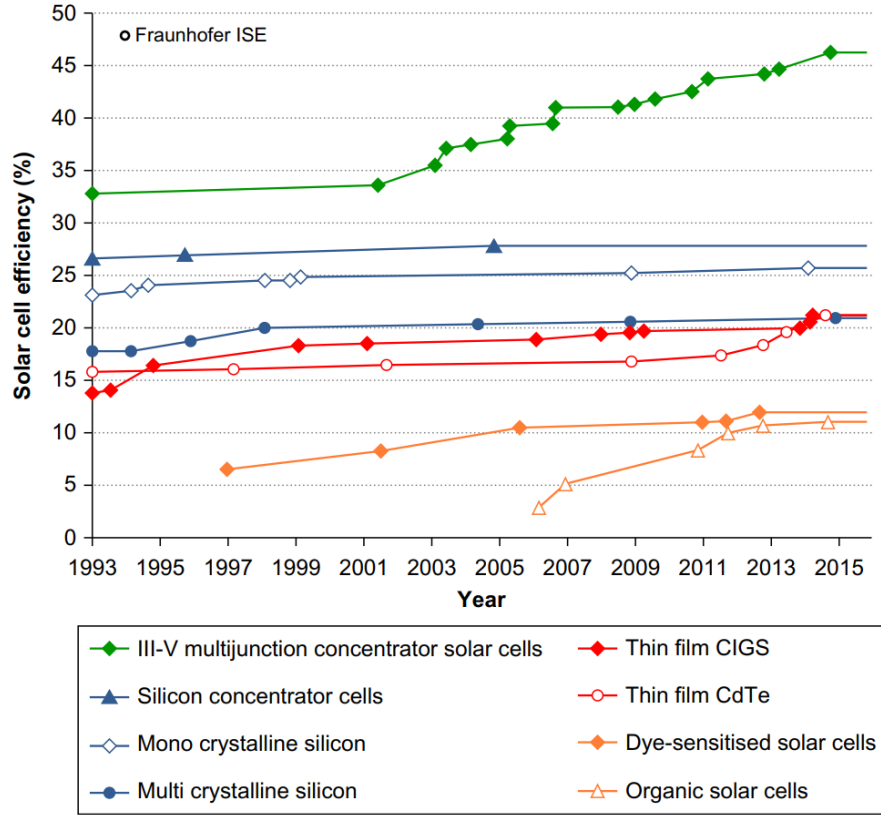


Figure 7: Photovoltaic Panel technologies and their highest laboratory efficiencies, graph of Simon Philipps, Fraunhofer ISE 2016.

Other technologies include Thin Film solar panels, which takes advantage of thinner body of junctions of a cell, thus creating a lighter and low-energy cost panel, with as much efficiency as a Mono-Si PV. Also, the most significant feature of the thin film technologies, is the flexibility of the panel itself, which provides the capability of standing in floating surfaces, such as the water. For this reason, many designs have been conducted for offshore thin film solar plants such as in [13], however we couldn't find real-world implementations of such ideas.

As described in section 1 of the current study, one of the general advantages of FPV plants, is the increase of the panel's efficiency due to lower temperatures of the surrounding conditions. More specifically, studies have shown a significant change of the panel's

efficiency, when the last is submerged under the water body. Several studies have explored the capabilities of the SP2, or Submerge Photovoltaic Solar Panel, with a good sum up of the results to be shown in [4], where the authors integrate the solar spectrum properties with those of the water body and solar panels. We know that the integral of total spectral irradiance is the irradiance  $G(z)$  in  $W/m^2$  which is expressed in the following equation:

$$G(z) = \int E(\lambda, z) d\lambda \quad (1)$$

Where  $\lambda$  is the wave length of solar radiation,  $z$  is the water depth and  $E$  is the amount of spectral energy coming from solar irradiance. In fig. 8, the solar spectral irradiance, absorption is compared with the depth of the water and thus we can extract the percentage of the absorbed radiation in function of the water depth.

Description	Symbol	Unit	Value								
Water depth	$z$	m	0	0.02	0.05	0.1	0.5	1	2	5	10
Irradiance	$G$	$W/m^2$	1004	837	692	645	507	443	380	286	211

Figure 8: Transmitted radiation as a function of water depth, courtesy of [4].

From the above, we can understand the significance of the water depth as function of the provided beamed irradiation. However, we need to also analyze the semiconductor's band gap energy as well as the cut-off frequency (or cut-off wavelength).  $E_G$  is the bandgap if this energy is higher than the band of the cell material, the rest of this energy is wasted to heat on the panel. On the other hand,  $\lambda_G$  is the cut-off wavelength of the solar spectrum from which the cell won't receive any number of photons, so the rest of the irradiation is not going to be useful for the cell, thus it is wasted also as heat.

Material	Ge	CuInSe <sub>2</sub>	Si	InP	GaAs	CdTe	a-Si	GaInP	Cu <sub>2</sub> O	Se
$E_G$ (eV)	0.62	1.05	1.09	1.22	1.42	1.45	1.76	1.88	2.1	2.2
$\lambda_G$ ( $\mu\text{m}$ )	2.0	1.18	1.14	1.016	0.873	0.855	0.704	0.659	0.590	0.563

Figure 9: Bandgap & cut-off wavelength for various panel technologies.

Based on those 3 properties mentioned in the 2.2-chapter, water depth, bandgap energy & cut-off wavelength, a very explanatory diagram of efficiency versus water depth is shown in figure 9, curtesy of [4], to interpret the efficiency variation in water depths, proving that submerge solar panels are not panacea in aspect of efficiency, thus we need to use the water body carefully to receive any increase in the efficiency of our solar park. For Mono-Si and Poly-Si panel technologies, the below graph shows clearly the advantage of the partially submerged solar cell, but no more than 5cm.

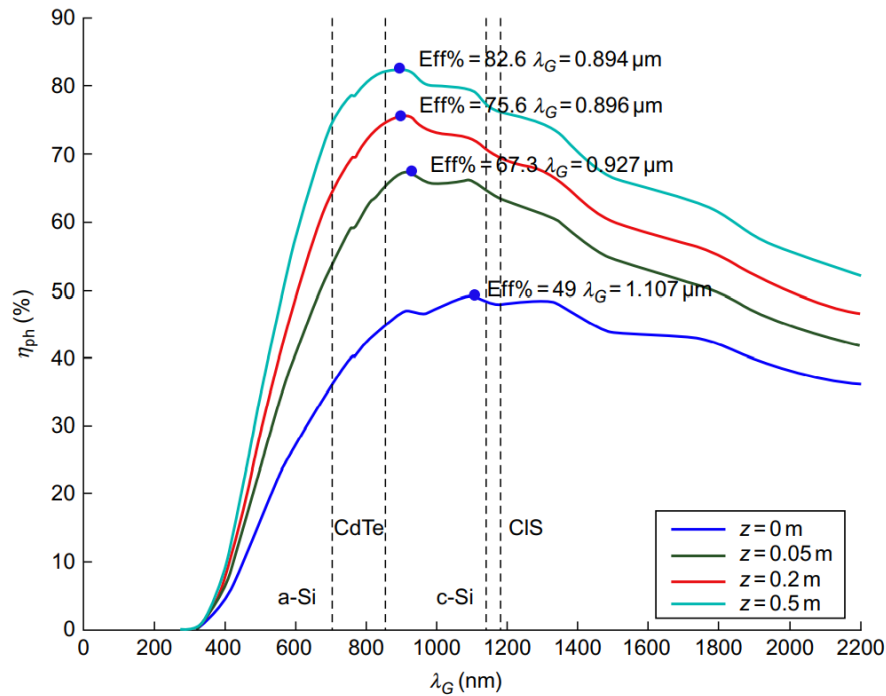


Figure 10: Photoelectric efficiency at different solar spectrum,  $E_G$  &  $\lambda_G$ .

Finally, we need to include in our research the phenomenon of the thermal drift on Solar Panels, which is a practical explanation of the panel's efficiency in function of the cell's

temperature. The classic thermal coefficient theory comes from the fact that open-circuit voltage decreases drastically from the rise of the ambient temperature, while the short-circuit current remains almost stable, thus the power and efficiency of the panels decreases. A widely used mathematical expression for the behavior of Power generation based on temperature is the following:

$$P(T_c) = n_{STC} * A_{PV} * G * [1 - k_p * (T_c - T_{STC})] \quad (2)$$

Where P is the power generated by the solar panel,  $n_{stc}$  is the efficiency of the panel on Standard Temperature Conditions,  $A_{pv}$  is the panel surface, G is the Global Irradiance on the panel,  $k_p$  the temperature coefficient in %/degrees Celsius &  $T_c$  the cell's temperature in a specific time. At this point, is significant to note that every producer and panel technology has its own  $k_p$ , so based on [4], in fig 11. we extract  $k_p$  statistics for every basic solar panel technology.

Technology	CIS	CdTe	a-Si	a-Si/2J	a-Si/3J	p-Si	m-Si	CIGS
No. of modules	8	6	4	6	14	12	12	13
Power range (W)	60–160	35–80	100–106	156–180	136–272	170–280	170–280	65–200
$k_p$ mean (%/°C)	0.353	0.250	0.200	0.250	0.226	0.438	0.444	0.342

Figure 11:  $k_p$  coefficient for various panel technologies and number of modules, courtesy of [5].

Admirable to note, is the high value of  $k_p$  for Silicon panel technologies, which indicates bigger loses from temperatures increases, especially in hot seasons. In FPV Parks, we can significantly diminish the temperature penalty in those panels, while keeping the overall costs of installation close to an LBPV, by using the water body for cooling purposes, idea which is further analyzed in the 4<sup>th</sup> chapter of this study.

Finally, in aspect of panel construction and proof, it is critical to remember that FPV structures, especially at offshore and coastal environments, are subject to high levels of humidity, dust, galvanic and electrolytic corrosion, even soiling sometimes from bird droppings etc., which is why more strict standards compared with LBPV regarding IP protection and external conditions, are implemented to ensure the proper function of the panels for at least 15 to 20 years span:

- IEC 61215 “Terrestrial photovoltaic (PV) modules - Design qualification and type approval - Part 1: Test requirements”.
- IEC 61730 “Photovoltaic module safety qualification”.
- IEC 62790 “Junction boxes for photovoltaic modules - Safety requirements and tests”.
- IEC 61215” Terrestrial photovoltaic (PV) modules - Design qualification and type approval - Part 1: Test requirements”.
- IEC 61701 “Photovoltaic (PV) modules - Salt mist corrosion testing”.

#### **2.4 Compatible Cables and Support Equipment.**

The cabling infrastructure technologies must ensure that the electrical cabling equipment of the FPV is waterproof and high-indurative in the external conditions. The same principle applies for the support and auxiliary components of the cable installations, which mainly is consisted of heavy PVC or highest endurance-XLPE insulations, flame redundant and halogen free for the safety of humans and animals. The operating temperature needs to be at from -20 up to 85 degrees Celsius. As expected, there are many standards that are in accordance with the aforementioned demands, most of them already used on ship electrical installations, marines and offshore platforms, with the most significant to be the following:

- IEC 60364-7-712 “Requirements for special installations or locations - Solar photovoltaic (PV) power supply systems”.
- IEC 60332-1 “Test of Fire Behavior & Flame Redundancy”.
- IEC 61034-2 “Ignitability and Burning Behavior of Materials & Products”.
- IEC 60754-1 & IEC 60754-2 “No corrosivity”. (Mostly in XLPE insulation cables).

Based on the previous compliances, many electrical cable manufacturers, i.e., Nexans, Hellenic Cables, General Cable, have standardized their own categories for DC solar panel cables, indicatively the FG16R16 category cable provides endurance and flexibility, while the FG21M21 is more rigid and simultaneously flexible choice, however more costly in comparison with the previous model. Also, worth noticing is Nexans’ distinct ENERGYFLEX Photovoltaic DC cables and General Cables PV-F1000. In XLPE categories, we got specific manufacturing models, which depend on the demands of the installation, such as the Medium-Voltage connection from the electrical substation to the grid via the sea floor or underground.

## **2.5 Switchgear & Protection Devices.**

In regard of protection gear for an FPV, a generic protection system between 20-1000kWp of power contains the equipment described below, following a power flow from the panels towards the inverter and the grid.

### **2.5.1 Fuse Disconnectors.**

Fuse Disconnectors, with internal gG type, cylindrical fuses for protection of each string in cases of panel equipment short-circuits. The rating depends always on the string’s parameters, which include, short-circuit current,  $I_{sc}$  and open circuit Voltage,  $V_{oc}$ , usually on the standardize value of up to 1000V DC. Complimentary, it is possible to add a Current Measurement Device on each string to monitor critical parameters of the string, although

this method is more costly due to more installation and equipment. Alternatively, we can use DC Circuit Breakers, which provide more flexibility, disconnection without the use of separate disconnect switch if is needed, as well as the same protection as the cylindrical fuse (of course, is a bit more expensive).

### **2.5.2 Bypass Diodes.**

Bypass Diodes, for protection in cases of high voltage drops to a panel from shading or potential damage (so called Hot-Spot Phenomenon). Usually, panel manufacturers include bypass diodes with every panel for this purpose, however, a major disadvantage is the voltage drop cause by the diodes, which slightly reduces the overall efficiency of the string.

### **2.5.3 Surge Protection Devices.**

SPDs (category T1 or T2) voltage surge protection equipment. Crucial protection devices in cases of lightning strikes. Taking advantage of a common ground topologies, SPDs will drive the lightning strike's overvoltage to the ground, protecting panels, cables and devices. Also, very significant is the installation of an SPD right before the connection of the strings to the inverters, to protect the inverter machine from lightning strikes, ideally category T2.

### **2.5.4 Surge Protection Devices.**

Main DC Switch Disconnectors, which are located in the end of every string topology, protecting the overall series & parallel connections of the PV to the MPPT socket of the inverters. In other words, this is the last protection measure from short-circuits and significant faults for every MPPT of the FPV park's inverter. Switch Disconnectors come in a variety of types and responses, topic which isn't described in this study, however we need to know that Switches are essential in the main DC side, as well as the AC side powered by the inverters.

### **2.5.5 Insulation Monitor Devices.**

Insulation Monitor Devices. Especially in the case of FPV Parks, insulation monitors provide significant information about the common ground state of the system. In Floating Photovoltaic structures, similar to most photovoltaic topologies, ground faults may occur between the platform and the electrical routes of the strings. These faults, depending on the insulation resistance between the live supply conductors and the earth-water body, may cause a fatal accident such as electric shock, fire mainly because of arcing, or potential damage of the equipment. IEC 61557-8 specifies the conditions under which warning signals should be generated, in order to maintain the safety of the system.

### **2.5.6 Residual Current Devices.**

Residual Current Devices. To protect ground-insulation faults from the AC side (by means of power delivered from the inverter), we need to install an RCD device to ensure the protection of the equipment and personnel. RCDs are obligatory measures of protection and are founded in every electrical installation, Home, Industrial and Renewable Energy Systems. In Photovoltaic applications, according to IEC 60364-7-712, if the DC side has not any isolation feature with the AC side, it is required to protect the AC side of the FPV with type B RCCB devices.

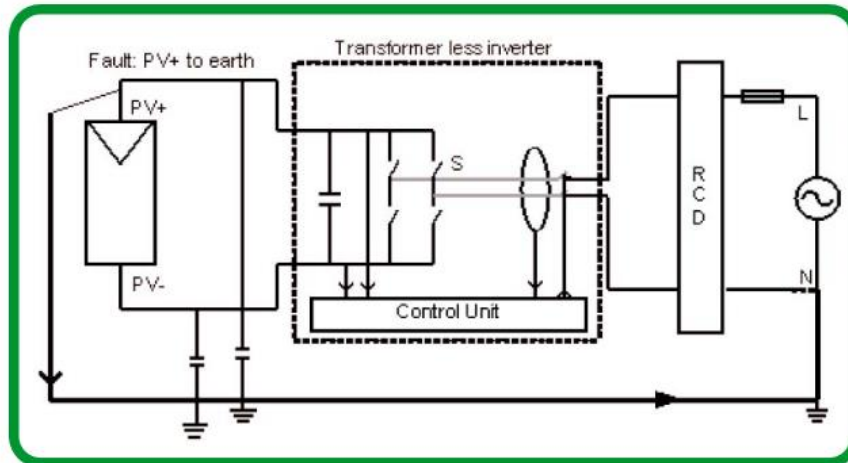


Figure 12: Circuit Diagram of a ground fault created by a photovoltaic array with TN-S grounding method, Guidance on Proper Residual Current Device Selection for Solar Inverters (white paper), Schneider Electric.

### 2.5.7 Main AC Circuit Breakers.

Main AC Circuit Breaker, capable of shutting down the inverter power delevrage in case of current faults and short circuits.

### 2.5.8 Main AC Load Switch.

Main AC Load Switch, which is capable of the immediate shutdown of the AC power grid delevrage. The same feature comes from the inverter itself, in cases of Panels or Grid Faults, however, we need to have a separate Main switch to ensure the total manual shutdown of the FPV system in cases of emergency. Also, worth noticing is that many manufacturers, like ABB, provide All in One Load Switches, which protect against overcurrent while providing the capability of switching High Loads (indicatively: ABB Tmax Series, Schneider NSX Compact Series).

## Application overview

Commercial system 20-1000 kW LV/MV

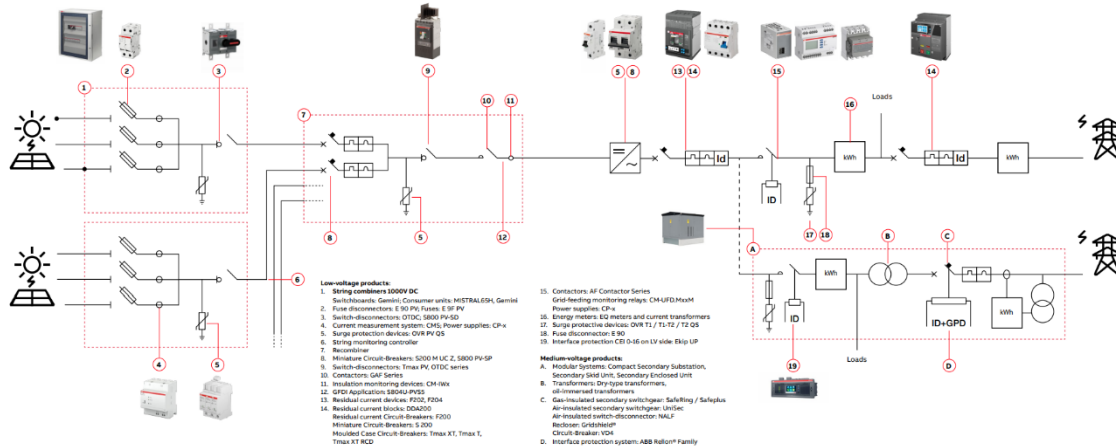


Figure 13: Diagram of Protection and Control equipment for a PV plant 20-1000KWp, courtesy of ABB.

The purpose of the above list was to introduce the reader to the essential protection and switching equipment for FPV premises. Keep in mind, that every manufacturer has its own models and types, however based mostly on global regulations i.e., IEC, UL, ROHS, the general features and properties remain the same. Furthermore, the equipment requirements change for produced power higher than 1MW. In the final chapter of this study, a model of 40 kW FPV is going to be presented accompanied with the essential equipment from the above list.

## **2.6 Inverters for FPV installations.**

There are 3 main categories of inverters, depending on the type of Photovoltaic Topology, power produced and the number of different panel tilt angle. Bellow, we follow a general description of the type of inverters, while we mention some examples of implementation in recent FPVs.

### **2.6.1 String Inverters.**

The most classic type of inverters, providing separate MPPT (Maximum Power Point Tracking) optimizer for every set of strings. Useful to remind, that every set of “string” can be comprised of many series-parallel panels, however there is a trade-off between the number of panels and the optimized power extracted from every set, as well as there is a limit in the maximum current an MPPT socket can tolerate. A very useful advantage of the sting inverter, is its capability to receive different voltages and currents from each string is connected, which is why is widely used even in high MWp plants with many different tilt angles. Also, their replacement and maintenance are easier than Central Inverters, which are mentioned below.

The range of power varies from 1-100 kWp, and the energy produced can be distributed to a) the grid (Grid-Tie Inverters), b) to storage systems i.e., battery or pumped storage (Storage Inverters, MPPT Battery Chargers) and c) Hybrid Inverters, a recent technology which combines storage and grid power distribution whenever is needed.

In FPVs, they are found in installations such as In Singapore inshore Projects [8] at fig.2, or at offshore projects by Swimsol in [11].

### **2.6.1 Central Inverters.**

Second on the market share are central inverters, All in One system, which deliver high amounts of power to loads or storages, similar to string inverters. Usually come in prebuilt structures, with all the necessary electrical equipment included, and require constant maintenance and inspections from expert technicians. Their main difference

compared to string inverters, is that only one MPPT socket is used with high current tolerance, which is why it is preferred for PV with the same tilt angle, such as rooftops.

In FPV cases, we can see them used from MWp Parks, such as the Huainan Project mentioned in previous Chapter 2.2 and in Fig. 5.

### **2.6.1 MMPT Power Optimizers.**

Devices which monitor each module individually and communicates with the rest of the modules to further optimize the energy production of the photovoltaic system. Even though every inverter typically comes with some MPPT sockets as described above, these MMPT algorithms receives only the voltage and current of the whole string-series topology, thus decides a current that optimizes the whole string, not every individual panel. MMPT Optimizers receive voltages and currents from all panels of the park, thus deciding altogether the MPPT of the whole topology. Even though it provides increased results in power produced, it is a high-cost investment with many compatibility issues. In the scope of this study, none of the FPV Park investigated where in use of MPPT Power optimizers.

## **2.7 Grounding Methods for FPV Parks.**

Grounding of the FPV parks constitutes a compulsory measure, to protect personnel, humans and wildlife (known as safety grounding), as well as to ensure the proper function of the FPV equipment (equipment grounding). Worldwide, there are a lot of grounding methods used for electrical installations, which depend on the nature of electrical premises, as well as the local regulations applied in each country. For most European countries, such as Greece, FPV parks are subjected to the IEC Standard 61892 “Mobile and fixed offshore units - Electrical installations”, in which grounding methods are elaborated.

Initially, it is critical to understand the possible earth faults than may occur in a FPV park, in order to monitor and prevent them. Initially, capacitive discharges between the panels and the ground is a classic phenomenon in photovoltaic installations, with recordings showing capacitance up to 50  $\mu\text{F}$  for a 100kWp land-based plant on rainy mornings [14].

Even higher capacitances can be created in lake textures, which means that high discharge arcing currents may be induced towards the ground or the water body, creating electric shock accidents and damage of significant equipment. Especially in cases of grounding to the water body, the path of current leakages can quickly corrode the metallic parts of the platform, via electrolytic corrosion, which is also a reason why most platforms are supported upon plastic mooring bases, as described in Chapter 2.1. The last problem described, may not be obvious, but many studies suggest that lake water have lower resistance/meter in comparison with concrete and land type of soils, hence an explanatory table from DEHN is provided in fig. 13.

Furthermore, leakage currents may occur from an unintentional DC ground fault, such as the damage of a cable sheaths, or the damage of a junction box, destruction of equipment etc. Usually, the currents created by these faults isn't enough to trigger the DC protection devices, thus if multiple faults happen, and those aren't cleared, very high currents will occur from the DC side to the ground, destroying gradually or immediately equipment and cables. Of course, in the FPV installations, where the most part of the platform is in contact with the water, it is possible that a current path can be created through the water, which in turn can shock passing by swimmers or animals.

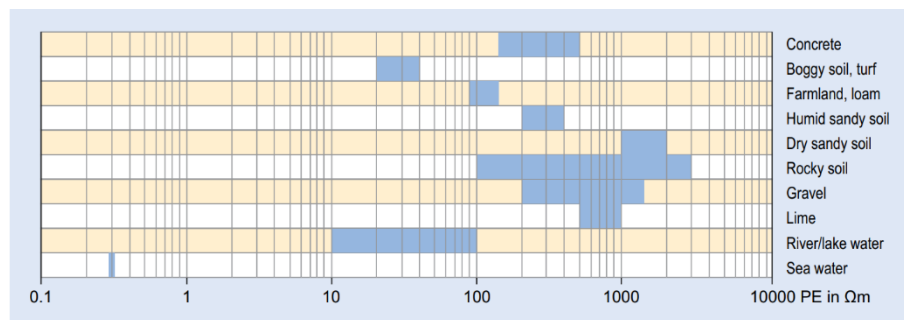


Figure 14: Typical Resistance ( $\Omega m$ ) for various types of soil, DEHN 2014, p.121.

Typically, FPVs for coastlines, lakes, reservoir and similar environments use Grounded Neutral methods (formally TN-S), in which the non-current conductive parts, such as the aluminum frame of the panels, are connected to a conductor cable (PE) with typical cross section of  $6\text{mm}^2$  to  $16\text{mm}^2$ , with similar protective sheath as PV cables described in Chapter 2.4. In turn, the radial network of PE conductors throughout the FPV park is connected to the main PE busbar of the FPVs inland electrical cabinet. Lastly, the main busbar is connected to an electrode at least 1 meter long, ensuring that any electrical fault that occurs, finds a very low resistance path to close the fault circuit. IEC regulations state that, especially in humid environments, resistance of the protection grounding should not exceed  $0.5\Omega$ , due to the fact that humidity lowers the resistance of ground faults. An indicative inshore DC-AC, TN-S distribution system is provided in figure 14. To further address the issue of leakages in the water body, IEC 60364 requires Insulation Measurement Devices (especially for non-isolated inverters) and type B RCCB devices, only applicable in cases of AC distribution plants, with their detailed function described in Chapter 2.5.

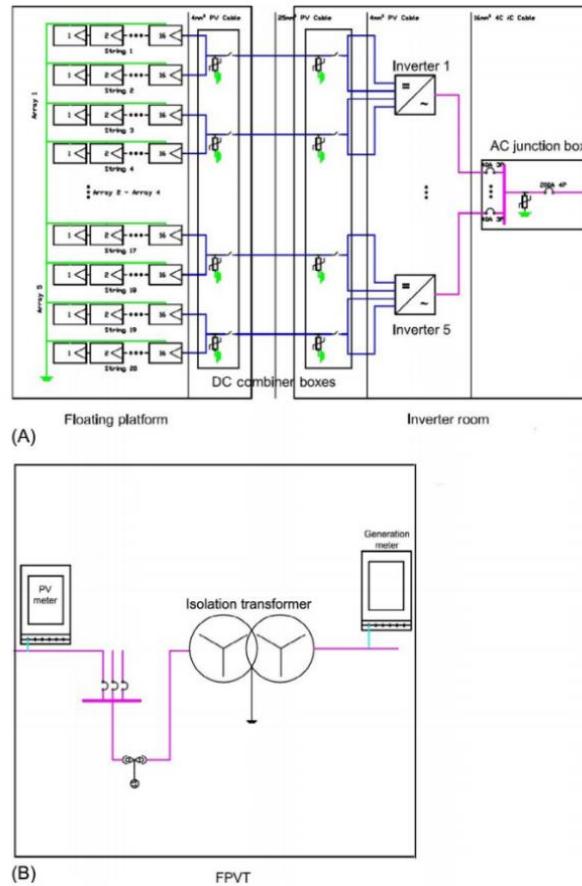


Figure 15: Typical electrical DC to AC distribution of a FPV with TN-S grounding system. Upsolar 100kWp FPV park, Singapore.

In cases of DC-DC distribution, we also need to provide sufficient grounding body for current faults. The solution is given by grounding the minus voltages of the park, creating a low-impedance path for the DC fault, similar to DC grounding methods used by large vessels and cargo ships. Again, to further avoid DC arcs and electrolysis, we will immerse the DC-grounding plate only in one part of the platform, at which all the PEN conductors from the strings will be connected. The part of grounding in one point connection is crucial to ensure that leakage currents wont flow from many parts throughout the platform to the grounding plate, for corrosion issues described previously. In fig. 15 we show a typical DC-grounding circuit diagram, with isolated inverters. Keep in mind, that isolation monitor devices are very significant in any Solar Panels installation above 20kW, independent of the power delivered to the grid.

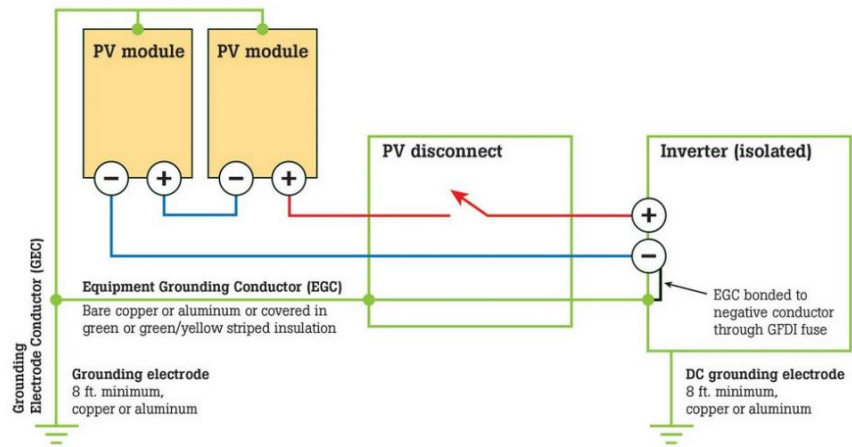


Figure 16: Circuit diagram of DC-Grounding method with isolated inverters, courtesy of Fluke.

## **3. Simulation of Performance Differences Between FPV & LBPV Parks In Crete, Greece.**

---

### **3.1 Introduction**

In the 3<sup>rd</sup> Chapter of this study, we will simulate 3 different methods of Photovoltaic Installations, 1 Land-Based Photovoltaic arrangement with 1 Inshore Floating-Photovoltaic and 1 Offshore of the same nominal power. Our goal is to find any performance differences, given that floating photovoltaics are installed in a very different environment than land-based, in aspect of meteorological ambient conditions, as well as structure. Moreover, we further analyze data selection, techniques and parametrization to efficiently simulate a performance analysis FPV Parks. Lastly, conclusions are made, disadvantages of our methods are described, and challenges in the field of FPV simulations are discussed.

### **3.2 Selection of Case Study Sites.**

The selection of a specific place for our FPV simulation defines crucial parameters such as the weather conditions, the type of structure for the support of the Panels/Equipment as well as the type of electrical distribution which is going to be used. In order to compare more efficiently the results of our simulation, 3 similar, 40 kWp PV Parks with AC power distribution is assumed to be installed in lake, sea and land respectively, in maximum distance of 15km between the furthest of those 3. Moreover, the installation sites were chosen by generic geological data and are set for simulation purposes only.

For the offshore unit, we need an area with low sea-wave heights, like harbors and coastlines in small gulfs, to reduce the effects of extreme weather conditions which would damage the structure and function of the FPV system. Furthermore, to avoid high electrical installation costs (wires, protection and control equipment, high-voltage transformers etc.), we need to place the park as much near the shore as possible, thus using small distances of

immersed cables and, possibly, housing the main electrical equipment and grounding to inland structures. Transmitting DC energy to inshore electrical cabinets diminishes capacitive and reactive losses, special type of cables and auxiliary routing protection, rigid and waterproof infrastructure. In addition, near-shore installations reduce the dangers of lightning strikes, high-cost of remote maintenance, and uses the shore to further utilize FPV infrastructures i.e., 1-axis tracking system with the use of rotation mechanisms [5]. Of course, each FPV project has its own goals and hence specific structural properties, i.e., FPV near petroleum platforms, which is very different than the previous criteria mentioned, however, in this simulation, we study a coastline offshore FPV for easiness of comparison.

Based on the abovementioned criteria, we chose the 3 different locations for our inshore FPV, offshore FPV and LBPV respectively. The locations were near with each other, in the same province, for proper comparison reasons. The exact selection of the sites is described below:

### **3.2.1 Offshore FPV. Souda Bay, Chania, Crete**

Bay of Souda is one of the biggest natural gulfs and harbor of the Mediterranean Coast. It has a coastline span of 15 km, with width which expands from 2-4km. For obvious reasons, Souda Bay is an ideal place for in-water activities and constructions, due to its very low wave heights and relatively less frequent wind speeds. The FPV would be located very close to the coast, providing platform paths for maintenance. The exact location was chosen to be near the small Island of Souda inside the bay, to match as closely as possible the meteorological and solar data with the other 2 PV comparisons, and to simulate the weather conditions for an offshore FPV. The location of the FPV provides relatively easy commissioning and connection to the grid, while is effectively surrounded by small land parts to reduce impact of the open sea waves.

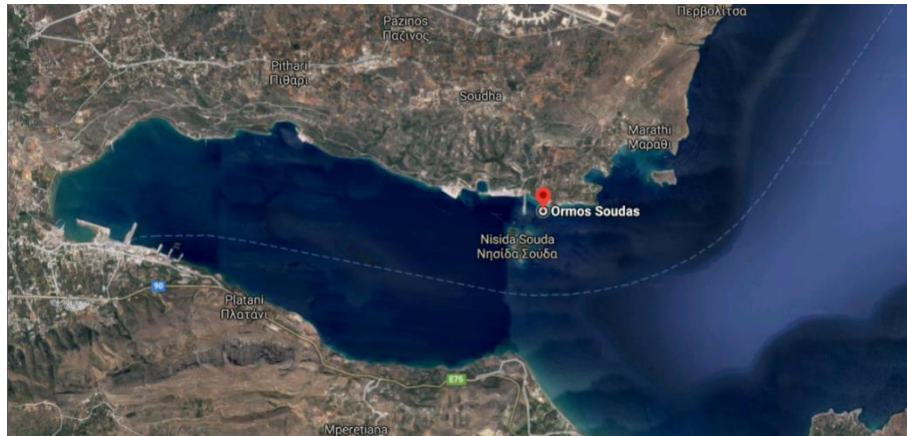


Figure 17: Location of the Offshore FPV plant in Souda Bay, Crete, Greece (via Google Maps).

### 3.2.2 Inshore FPV. Souda Bay, Chania, Crete

The Agia Lake Reservoir in Cydonia province, Chania, Crete is a fresh water artificial lake with open fields and thick vegetation around it, just 10 km away from the city center. With water surface about 450km<sup>2</sup>, it's an ideal place from the installation of an inshore FPV, close to main Grid connections and Substations of Medium Voltage. The freshwater lake provides a fluid environment, with increased humidity and decreased ambient temperature in the summer, adding cooling support for the photovoltaic panels of our small park.

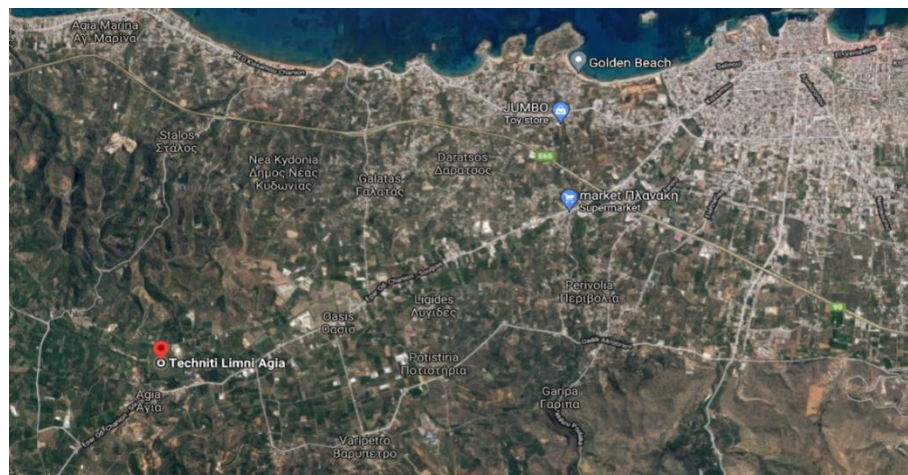
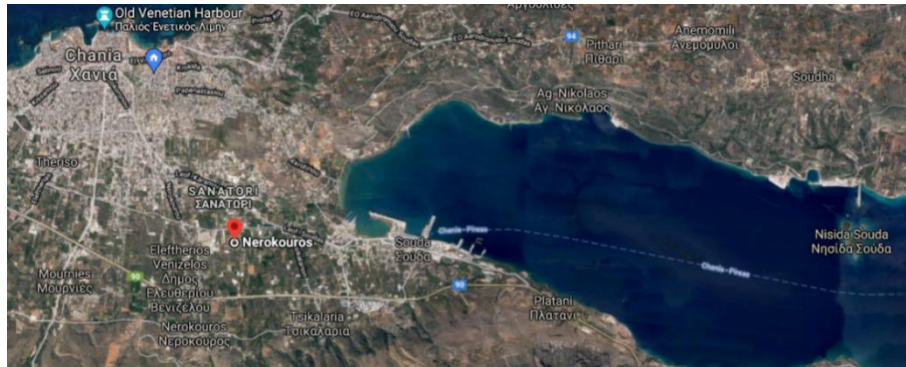


Figure 18: Location of the Inshore FPV park in Agia Lake, Crete, Greece (via Google Maps).

### 3.2.3 Land-Based PV, Nerokouros, Chania, Crete

The land based photovoltaic system is supposed to be located in a generic site for an PV construction, between the inshore and the offshore places. All 3 PV remain in the city of Chania, in order to simulate the comparison of those 3 cases with similar as possible weather and solar conditions.



*Figure 19: Location of the Land-Based PV Park in Agia Lake, Crete, Greece*

For all the PV installations, we simulate the same Panel Tilt and Azimuth Angle, giving that all the installations have similar solar irradiance curves during the same days, although they are not expected to match identically, due to small cloud forms and other stray occurrences of a typical day. In the next chapter, it is explained in very detail, sources and methods of acquiring meteorological data in order to create a highly accurate typical meteorological year.

To validate the similarity of all 3 solar data, the overall POA Irradiance received from each system were calculated, given that all 3 systems have the same azimuth and tilt angles, and the results are given in the next table:

PV System	Yearly POA Irradiance (KWh/m <sup>2</sup> )	Total POA Irradiance Received from the System (KWh/y)	Percentage Difference from LBPV
Inshore	18351	4330468.98	-1%
Offshore	18468	4358078.64	-2%
Land-Based	18129	4278081.42	-

Figure 20: Total POA Irradiance Received from Each Case Study PV Model, from simulation results.

### 3.3 Significant Parameters Distinguishing FPV from LBPV Installations.

In order to evaluate possible differences in the efficiency of Land-Based PV and Offshore/Inshore FPV, it is essential to understand the basic parameters distinguishing these 2 installation methods, which have an influence on their overall performance.

Initially, the most obvious difference is the surrounding environment, which is analyzed also in Chapter 1 of these study. In the open sea, we can notice much more humidity than inland, lower ambient temperatures and frequent high wind speeds, parameters which have a great impact on the overall cell temperature of the Photovoltaic Panels, and in turn in their efficiency. In classic LBPV installations, the expected cell temperature of the panels is often calculated only by the recorded air temperature up to 2m from the ground (also known as Dry Bulb Temperature or abbr. T<sub>2m</sub>). However, air temperature can also be affected by humidity, wind speed and air pressure, which means we need a more detailed model of ambient temperature. To integrate all the above-mentioned parameters, we use the following equation implemented by Jacobs et. al. in [15]:

$$T_A = T_{ab} + 0.33 * p_v - 0.7 * |v| - 4 \quad (3)$$

Where T<sub>A</sub> is the apparent temperature. T<sub>ab</sub> is the dry-bulb temperature or air temperature, p<sub>v</sub> is the vapor pressure in hPa. Vapor pressure, is calculated via the following equation:

$$pv = \exp \left( 1.8096 + \frac{17.69D}{273.3 + D} \right) \quad (4)$$

Where D is the dew point temperature which is in turn calculated by:

$$D = T - \frac{100 - RH}{5} \quad (5)$$

RH is humidity and T the air temperature at 2m meters height from the ground (T2m). After calculating the ambient temperature, we need to integrate the effects of the last on the panel's cell temperature, using the following correlation provided by Sandia National Laboratories, Albuquerque, NM. [16]:

$$T_m = GHI * (e^{a+b*WS}) + T_A \quad (6)$$

Where Tm is the module temperature, GHI is the solar radiance incident on the panels, a & b are parameters depend on the module construction (in this study, we assume glass/cell/polymer sheet panels) and their values are a=-3.56 and b=-0.750.

Another factor that we need to consider, is the tilting angle of the photovoltaic panels. The variance in the tilt angle, consciously would mean that the panels change their angle of incidence to the sun, thus reducing or increasing their absorbed irradiation. In offshore and inshore FPV installations, waves are moving the panel's platform, thus creating a fluctuation with frequency and height with random distributions, depending on the wave heights, the water body area (engulfment, or open sea etc.), the wind speed and its duration. Many studies have been conducted to find a correlation between the water body behavior and the waves frequency and height, however, it is widely accepted that the creation of waves is a complex and multi-parameter problem, difficult to be forecast or simulated [17] . In this study, it is assumed the wave heights changing the tilt angle of the photovoltaic panels with

a Poisson distribution, due to the memoryless nature and complexity of the sea waves, especially in the open sea, as well as from meteorological data acquired, which have shown that wind speed rates are following a generic form of Poisson Distribution throughout a typical year. By analyzing the wind speed rates for every PV installation site in a one-year span, we can further confirm the previous statements by the figures below:

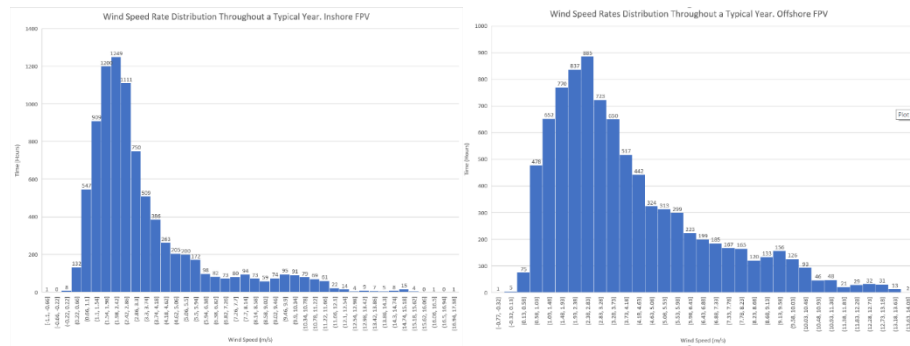


Figure 21: Wind Speed Rates Distribution recorded in a Typical Meteorological Year for Inshore FPV (right) and Offshore FPV (left), data source: PVGIS.

From the figures above, we can easily notice the differences in the wind speed occurrences in a whole year, results expected due to the different sites the data where recorded (Inshore FVP, Limni Agia vs. Offshore FPV, Souda Bay). The inshore site has a record of low rates of wind speed for the majority of the year, with most hours of a year be recorded in 1-5,5 m/s or 1-3 Beaufort, while the offshore site records a wider range of wind speed, about 1-10 m/s or 1-5 Beaufort. Assuming that the tilt of the panels changes in accordance with the wind speed, the tilt angle change will also be modelled as a Poisson distribution with mean value  $\lambda=5$  for the inshore FPV and  $\lambda=14$  for the offshore FPV, which practically means that every 1 minute, the tilt of our panels will change with Poisson distribution with  $\lambda=5$  &  $\lambda=14$  for the inshore and offshore FPVs accordingly. A very detailed wave model, applied mostly in the open seas, can also be created by using the JONSWAP model, giving the frequency of the waves, their amplitude and their duration we can extract a very precise model of the wave height. However, this task is not included in the current study due to limit of wave and

climate data for the open seas. (Extended analysis of data handling for the JONSWAP spectrum is described in [1] & [18] ).

Moreover, the Angle of Incidence (AOI) is crucial parameter deciding the direct beam irradiation received in a photovoltaic module (DNI). In LBPV installations, AOI is a linear curve expanding through the days of a year, with no variations or fluctuations, given that the fixed angle of the panels receives the arrays of the sun, which changes staidly altitude as the day comes and goes. In a floating structure, the AOI is constantly fluctuating with a variance described in detail in the next chapter.

Lastly, we need to mention the differences in albedo levels as well as soiling factor. At sea, there are relatively less obstacles and structures capable of reflecting extra irradiation on the panels, compared to land, where albedo can reach much higher values due to urbanization, snow and clouds from air pollution. Furthermore, water absorbs much of the irradiation coming from the sun, in contrast with white-color concrete surfaces in a city. Hence, a low albedo coefficient value is considered for both the inshore and offshore FPV systems (albedo = 0.2), while for a rural area is ranged between 0.4 and 0.6 [4]. In regard of soiling levels, it is known that inland PV installations can be soiled by dust, rubbish and bird droppings. Excluding the dust, inshore and offshore FPVs are more prominent to bird droppings, algae and salt water stains that can be easily developed in the surfaces of the panels and their support equipment. Considering the previous factors as well as similar studies on this matter [14] [4] [8], we will consider SF=0.94 (Soiling Factor) for the inshore FPV, SF=0.89 for the Land-Based and SF=0.83 the Offshore Photovoltaic.

### **3.4 Selection of Simulation Tools.**

The selection of a suitable simulation tool requires a deep understanding of our model parameters, their characteristics and the field of calculations needed to be done, so as to produce a viable result. In today's market, we can find many simulation/calculation tools for Photovoltaic Performance Analysis, with each of them having its own advantages and disadvantages. For this study's simulation model, 3 main PV calculation tools/libraries are used, in order to ensure proper function and results of our model.

The initial simulation trials were done using the PVSyst program. PVSyst, is a classic and very accurate simulation program, capable of modeling any scale of PV installation with many extra features, such as distribution types, 3D modeling of the photovoltaic premises, bifacial module simulation, use of real measured data for both inverters and photovoltaic panels. However, it cannot support dynamic changes of the panel's azimuth and tilt angles, due to its calculation algorithms which use a specific AOI (Angle of Incidence) per hour. As mentioned in section 3.3, the AOI of an FPV is constantly changing, especially at offshore installations, where waveforms are frequent with significant altitude. Thus, we will use PVSyst for generic calculation methods, such as optimized angle & azimuth for our 3 PV locations, panel arrangement calculations and selection of efficient inverters for our model.

Next, the search for more parametrizable tools guided us to MATLAB tools and more specific, to PV\_LIB Toolbox. PV\_LIB Toolbox is an open-source library developed by Sandia National Laboratories in 2004 but have since been offered as open-source software projects and have grown significantly from contributions from an active community of users. More specifically, this toolbox provides well documented MATLAB functions of a wide range of PV calculations, which can be further developed or modified, according to the topology of the PV calculated. In other words, we are capable of modifying and calculating separately, every parameter of the PV performance model, which is suitable with our desired modifications in Ambient Temperature, Variable Angle of Incidence, Cell Temperature and Meteorological Data. Furthermore, we can increase the sampling ratio of our results, hence providing detailed data of a whole year of operation, using existing simulation tools of MATLAB. Useful to note, that the comparison of PVSyst and PV\_LIB Toolbox has been conducted in previous

studies and the results showed about 5% deviation from real data recorded [19]. Lastly, similar capabilities are provided in the NREL SAM modeling tool, however PVLIB was chosen due to its better flexibility.

### **3.5 Meteorological Data.**

The meteorological data used in this case study were based on the Photovoltaic Geographical Information System (PVGIS), which is capable of providing very accurate climate data from all around the globe and simultaneously irradiation data, which includes the classic 3 components of Global Irradiation, Beam Irradiation & Diffuse Irradiation. The results are free to download and have a sampling rate of minimum 1 sample per hour.

The most significant feature of this tool however, is the Typical Meteorological Year Tool (TMY Tool). With TMY Tool, PVGIS analyzes meteorological data from 10 years or more, to finally generate a file with the most “typical” 12 months of the decade (or 12-year span) selected for a specific site, thus creating a typical meteorological year. This statistical tool assists on creating a very accurate dataset of hourly values for the basic climate parameters which include: Irradiance Components (GHI, RHI, DNI), Temperature up to 2m from the ground, Humidity, Air Pressure, Wind Speed and Direction of Wind. TMY tools can be found also at other Photovoltaic Information systems, such as NREL. In addition, PVGIS optimizes the azimuth and tilt angle for a photovoltaic installation, given a specific location on the map, with very good accuracy.

Having the necessary meteorological data, as well as coordinates, altitude and irradiance components, we are able to simulate our performance models with excellent accuracy, which can be even more accurate by interpolation of the hourly data samples, to 1-minute data samples. In the next chapter, we will further analyze data handling methods and models used to sufficiently model our case studies.

### **3.6 Simulation Process & Results.**

In our simulation process, we used several functions of the PV\_LIB Toolbox to simulate efficiently the performance of our PV systems. As an assistance feature, PV\_LIB provides example scripts of PV performance models, which are divided in many MATLAB functions, each one of them producing a specific simulation result of our simulation. We will divide this chapter of our study, based on the steps used for the performance simulation.

#### **3.6.1 Definition of the PV systems.**

In the initial part of this simulation, we defined the basic electrical configuration of our models, which contains the type and model of the inverter used, the photovoltaic panels producing DC power, the series and parallel topology, as well as the azimuth & tilt angles of the system. For the inverter part, we chose the KACO Blueplanet 40.0 TL3 M1 480V model, which contains 3 MPPT strings, maximum voltage of 1000V DC, max current rating of 36A for all the strings. All the parameters necessary for the equations of our model were extracted from the ECE Inverters Database, which was provided by PV\_LIB library.

The photovoltaic modules used were Sanyo HIP-225HDE1, classic modules of 225Wp nominal power production in STC,  $V_{mpp} = 33.9V$  &  $I_{mpp} = 6.64A$ . The extra parameters were also extracted from the Sandia Module Database, provided by the PV\_LIB toolbox. The modules have a topology of 9 parallel strings of 19 in-series modules, totaling a productive power of 38,491Wp. As mention in previous sections, all 3 case studies used the same topology and power for their PV systems, for easiness of the comparison procedure.

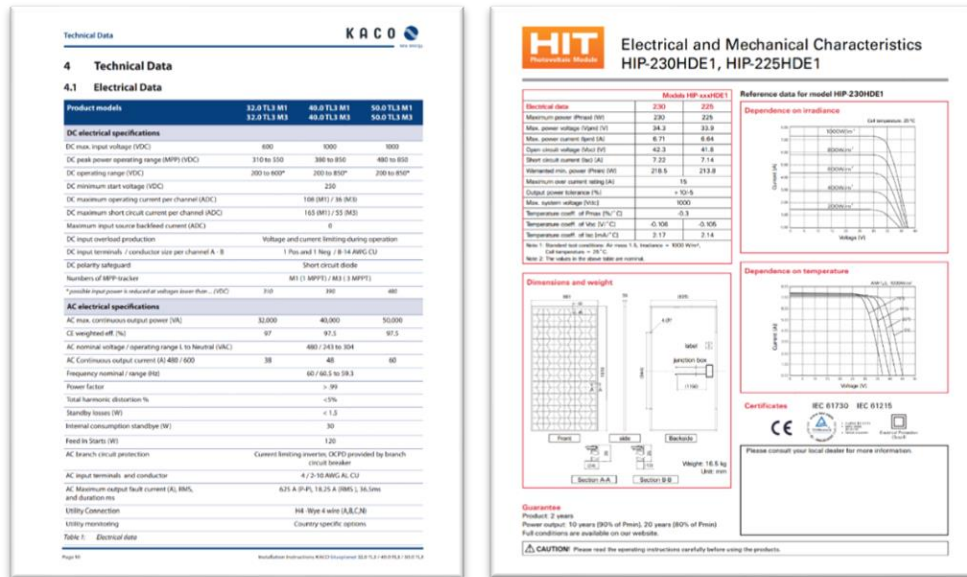


Figure 22: Case study selected Inverter Technical Data & Specifications, courtesy of KACO (Left) and PV modules Technical Data (Right), courtesy of HIT.

### 3.6.2 Definition of Coordinates & Surrounding Characteristics.

As mentioned in previous chapters, the difference of the environmental surroundings in each PV case can improve or undermine the performance of the system as a whole. The case study sites were selected closely between each other to provide similar solar data while serving their own purpose as inshore floating, offshore floating and land-based PV systems accordingly (The exact coordinates are described in Chapter 3.2). Using PV\_LIB toolbox *plv\_emphemeris* function, we manage to calculate the exact sun position, altitude, azimuth & AMx parameter regarding air mass. By adding the data of temperature & pressure recorded, we manage to have even more accurate external conditions influenced by our 3 locations. The results were further confirmed comparing the sun position created in the MATLAB script, with [www.suncalc.org](http://www.suncalc.org). In addition, the albedo of each site was considered, given than based on [1], the albedo of the water body is approximately 0.1, compared with the albedo of a rural area which receives values from 0.2-0.4.

With all the location & surrounding characteristics integrated, it was time to calculate the diffuse components, coming from the water body/ground and the sky, using the Klucher and Liu-Jordan anisotropic model, given in [20], which determines the sky diffuse irradiance using the GHI, DHI, sun azimuth and surface tilt & azimuth angle. For the ground reflectance calculation, we use a model presented by Loutzenhizer P.G. et. al. in [21] which takes into consideration the GHI, the Surface Albedo for water and ground accordingly and the tilt of the module's surface.

### **3.6.3 Integration of Irradiance and Climate Data.**

In the next part of this analysis, Irradiance and Climate data were integrated to our model, step necessary to extract parameters, such as sun position throughout the year and irradiance curves. Initially, the preferred sampling frequency is created to match the data described above, given that the TMY data used are provided in hourly values from the PVGIS system. In this case study, to efficiently model the PV parameters, it was decided that the sampling process is converted to 1 sample per minute, via interpolation of the given 1-hour sample data. To achieve this without deforming our data set, cubic spline interpolation algorithms of MATLAB were used, a classic and widely used solution on those cases.

Useful to note, that 1-minute interpolation provides more accurate metrics and supports the addition of deviations in array tilt angles, which practically means that the AOI of the panels will change constantly with a rate of 1 recorded deviation per minute, hypothesis very accurate since the wave formations don't change the tilt of a buoyant body with high frequency [17]. All in all, tilt variation with Poisson Distribution is induced in our model, a simple yet significant addition to the FPV model. Comparison of the DNI irradiation components between the LBPV and FPV panels is given in the following figure, to further understand the differences in the irradiation received from the panels due to the AOI changes.

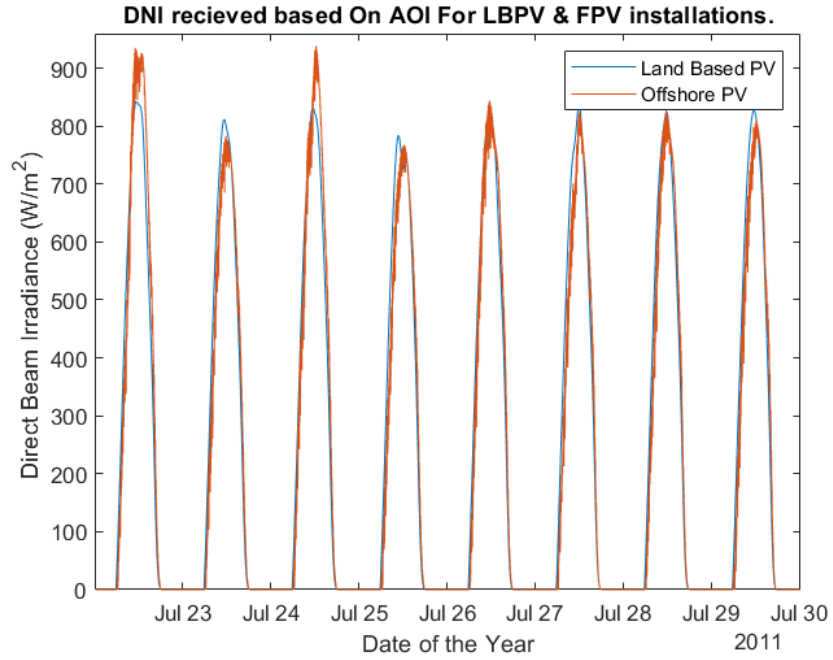


Figure 23: DNI irradiation received by Land Based PV and Offshore PV.

Next, it was time to calculate the Total Plane of Area Irradiance on the panels (POA), which is given by the following equation:

$$POA = DNI * \cos(AOI) + DHI_{\varphi} + RI_{\varphi} \quad (7)$$

Where AOI is the angle of incidence, DNI, DHI & RI is the direct, diffuse & reflected irradiance components accordingly, on a tilted surface.  $DHI_{\varphi}$  &  $RI_{\varphi}$  are given by the PV\_LIB toolbox functions which are described in the previous chapter. The differences between the LBPV Plane of Array Irradiance and the offshore FPV system are given in the following figure:

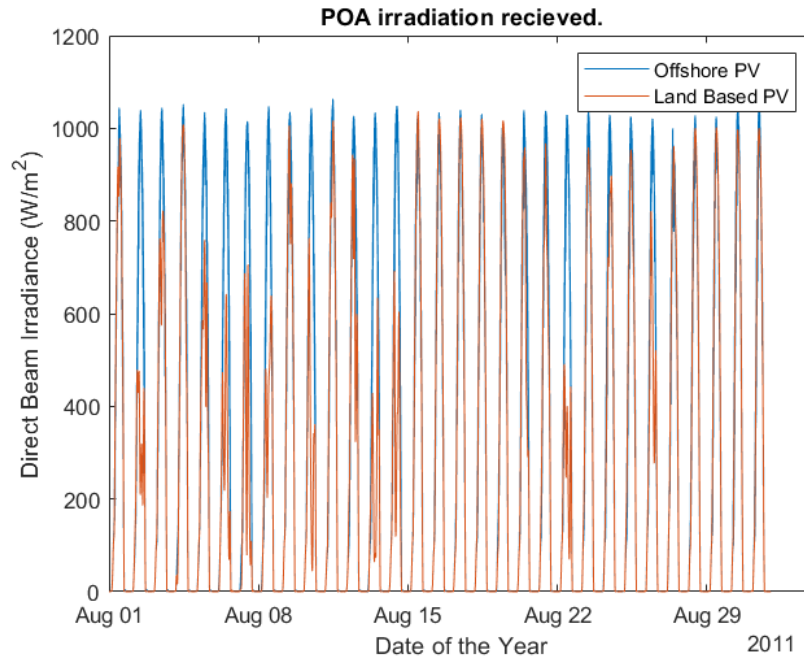


Figure 24: POA irradiation received throughout a Typical Month (August).

As we can see from the figure above, the POA differences between the 2 systems are not significant, result expected due to the selection of neighbor sites for this study. However, as also shown to DNI diagram, POA diagrams shows a noticeable tilt fluctuation of the FPV construction which decreases the overall irradiance received from the panels.

### 3.6.4 Calculation of Module Temperature.

Cell temperature and module temperatures are 2 very associated terms which provide significant details about the temperature in which the modules, or the cells within them, are producing energy. As it described in equation 2 of this study, the classic nominal power calculation equation provides us with clear evidence that temperature can significantly increase or decrease the performance of the module, thus it is crucial to add this specific parameter in our simulation.

Many studies have been conducted throughout the years to integrate the air temperature in the panel's performance, with confirmed metrics shown that high temperatures decrease significantly the performance of the modules in a hot weather condition. In this study, the SAP Cell Temperature model [16] is selected to elaborate more parameters regarding module construction characteristics, wind speed, POA and  $K_p$  coefficient all of them described in detail in section 3.3. The results are depicted in the figure 25:

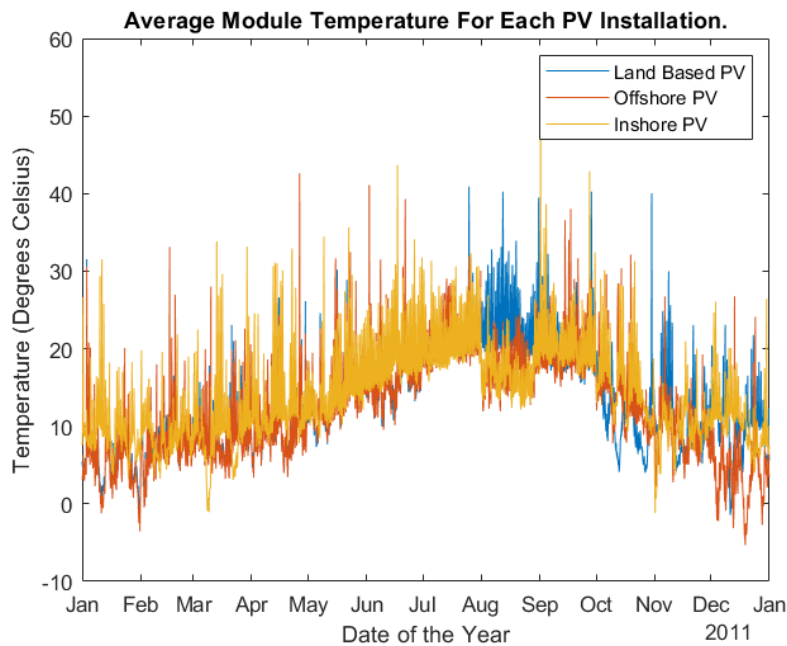


Figure 25: Cell temperature throughout a Typical Year for each PV system.

From the above diagram, it is shown that the FPV modules temperature is lower compared to the LBPV, for the most part of the year, and especially in summer and spring months where as it turns out, the produced energy is much higher than the LBPV, result of the high humidity, fluid environment of the offshore and inshore installations. However, the increased thermal capacity of the water body also means that the temperature of the photovoltaic modules will be higher than those on land on some occasions, especially from mid-autumn to winter months, thus reducing the FPV performance in considerable levels compared to the LBPV.

### **3.6.5 Calculation of Module's I/V Performance.**

After integrating climate, module and solar data, it was time to create a specific I/V performance model which takes into consideration a) the spectral loss of the PV system (described in Chapter 2.2 of this study), b) AOI losses, c) the effective irradiance reaching the modules and d) the internal losses cause by the structure of the panels. This model is described in very detail at the website of PVPMC, Sandia Laboratories and is provided in the PV\_LIB toolbox. Then, we can calculate accurately the DC production of our arrays, given a rich data of climate, solar, and module parameters, while accounting for any possible losses induced from the DC array itself.

Furthermore, acknowledgement of DC losses due to panels mismatch or equipment resistance is very significant, especially in high power PV plants which are connected with many modules (module diode voltage drop) and distant cables. In our 40kW plant however, the loss of power cannot exceed 0.01%, given that total cable distance is approx. 100m for each MPPT string of our 3 MPPT-inverters (copper resistance =  $0.017\Omega/m$ ), which further means that DC losses are negligible for our case.

### 3.6.6 Calculation of DC-AC Conversion & Overall PV Performance.

In the final stages of our simulation, we use the Sandia Grid-Connected Photovoltaic Inverter Model, fully described and parametrized in the PV\_LIB toolbox, to model the AC energy converted by our Inverter. Our 40 kW parks are expected to produce approximately 1500-1700 kWh/kW annually, which means that  $1500\text{KWh}/\text{KW}\times 40\text{KW} = 60\text{ MWh}$  per year.

PV System	Coordinates Lon. /Alt.	Tilt Angle (Degrees)	Azimuth Angle (Degrees)	AC Power Produced Annually (KWh)	KWh/KW Annually	Angle Variations (Degrees)	Efficiency Difference from Land- Based PV
Inshore FPV (Limni Agias)	35.476/23.933	30	135	60276	1565.98	5	4%
Offshore FPV (Souda Bay)	35.49/24.15	30	135	60847	1580.81	18	5%
Land-Based (Nerokouros)	35.48/24.04	30	135	57829	1502.40	-	-

*Figure 26: Basic characteristics and results for each case study, AC Power produced is extracted from our simulation analysis.*

Executing all the previous steps in our simulation produces 3 different results of PV performance regarding the LBPV, the Inshore FPV & Offshore PV. These results contain the recorded power production of every system, solar & climate conditions, various equipment parameters and analytics about the behavior of every one of the studied PV systems. Indicatively, annual recordings, regarding AC Power produced in a span of a typical year, and the recorded average module temperature in a daily base are provided in figures 27 & 28 accordingly:

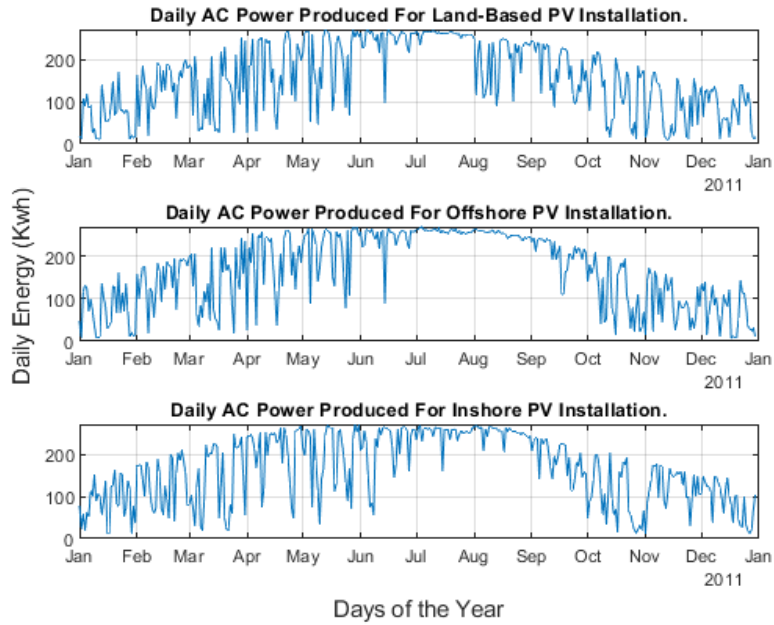


Figure 27: Simulation Results of Daily Energy Produced by Each PV System in a TMY.

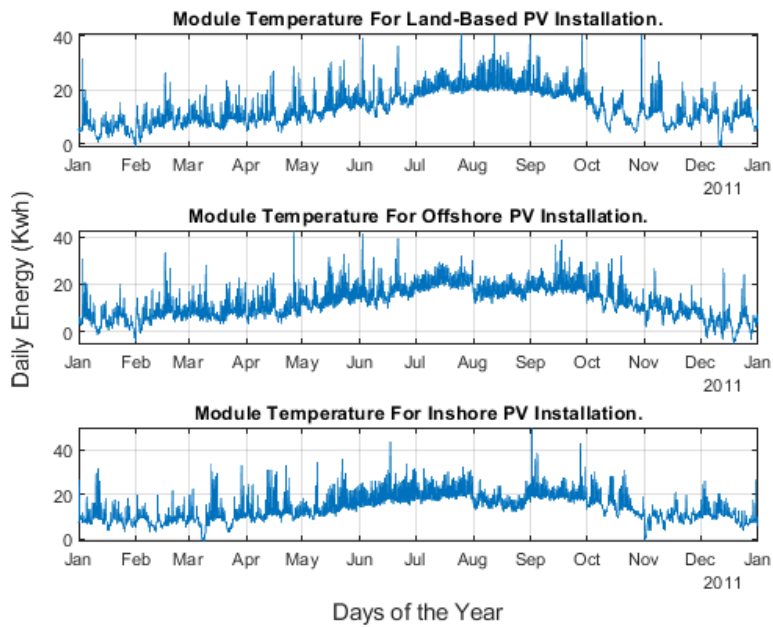


Figure 28: Simulation Results of Module Temperature Recorded in a TMY.

As we can see from the results above, there are substantial differences in the production of the PV Parks, mostly in the summer months, where the temperature of the water body decreases the overall module temperature, thus the production is more efficient. In the rest of the months, we can see minor changes in the overall production, which may be result of different weather conditions on each installation site.

In the case of the module’s temperature, we can see several noticeable differences occurred in the summer and the autumn period, where the FPV module temperature is significantly lower in comparison with the LBPV. However, we will also see the opposite effect happening in the winter months, where the water body thermal capacity keeps the FPV modules temperature above their LBPV counterpart, decreasing their overall efficiency on those periods. As we will see in figure 29, the overall energy production is impacted by the temperature fluctuation throughout a typical year, however this doesn’t mean that FPV parks are only benefited from the water body, instead in many of the winter months, the FPV systems provided substantially less energy than the LBPV park. The results of produced energy per month are shown below, so as to provide a better understanding of the FPV models behavior in contrast with the LBPV model.

Month	Land-Based 40KW (KWh)	Inshore FPV 40KW (KWh)	Inshore FPV Efficiency Difference from LBPV	Offshore PFV 40KW (KWh)	Offshore FPV Efficiency Difference from LBPV
Jan	2041.5	2645.9	23%	2170.9	6%
Feb	3953.1	3760.7	-5%	4085.2	3%
Mar	3911.4	4160.4	6%	4146.9	6%
Apr	5308.6	6337.7	16%	5647.9	6%
May	6293.6	6110.7	-3%	6816.6	8%
June	7494.0	6510.7	-15%	7343.5	-2%
July	8140.7	7783.6	-5%	8069.5	-1%
Aug	6201.9	7831.4	21%	7849.4	21%
Sept	5481.7	5681.6	4%	6294.5	13%
Oct	3901.0	2989.0	-31%	3505.0	-11%
Nov	2443.0	3777.5	35%	2767.9	12%
Dec	2658.9	2686.9	1%	2149.4	-24%

Figure 29: Monthly Energy Produced by Each PV Model.

The monthly AC Power production is very interesting to be commented. Expect for the cases where photovoltaic panels show minor differences in the efficiency of energy produced, significant differences are noticed in the months of January, April, August, & November where both inshore FPV and offshore FPV show an increase from 6%, up to 35%! However, as we can see in the months of February, June & October, there is also a high decrease of energy production compared with LBPV park, result expected based on the previous theories regarding the water body thermal capacity which has great impact on the overall ambient temperature on the site of the FPV installations. Of course, we should note that the influence of tilt variation, albedo and soiling factor differences also have an impact on the overall performance on each PV system separately, however, it is safe to say that each FPV installation has its good & bad months of energy efficiency, which is the reason why the overall production of the FPV models isn't changed substantially.

## 4. Epilogue, Conclusions & Future Trends.

---

The main purpose of this study was to appoint the major characteristics of the Floating Photovoltaic Installations, their properties from the mechanical to the electrical part, their pros and cons compared to the classic Land-Based PV installations, and to further simulate their performance differences by comparing 1 FPV case study at marine environment, 1 FPV at inshore fluid environment & 1 classic inshore PV, all modeled with real recordings and real solar production equipment.

In aspect of performance analysis, the selection of island of Crete, Greece was a choice which offered all the different installation scenarios, with very close distance between each other for solar data similarity. For this set of simulations, we found minor differences in favor of the FPV installations (5% increase compared to LBPV installation), which, however, don't provide a strong advantage compared to the classic LBPV installations in aspect of efficiency, and thus overall energy produced in an annual base.

However, with much lower cost and mechanical apparatus than LBPV, a very effective 1-axis tracking system can be constructed, especially at nearshore FPVs. such as the pattern designed in [4] & [22] , and increase the overall energy extracted by 20%. Furthermore, a viable solution is the permanent cooling of the panels via WVC (Water Veil Cooling) systems, using the water from the lake/sea via integrated pumps as shown in the following figure. The last idea, though, has a disadvantage of draining significant amounts of energy, always depending upon the FPV structure and rated power.

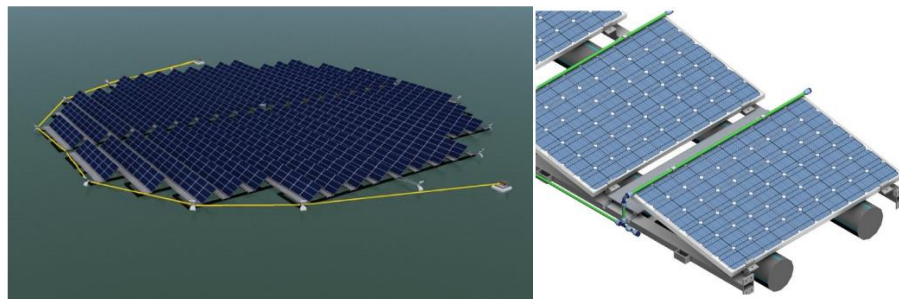


*Figure 30: 1 Axis Tracking & Water Veil Cooling Design for FPV Parks, courtesy of [5].*

The effect of lower ambient temperatures in the wide lake and sea areas, may do not offer many advantages in the Mediterranean climates, however, its results may be better for constantly hot areas such as African Countries, or the opposite, Northern Countries, such as the Nederland's or in Canada, where simple module-fixed FPV construction, as in our simulation, provide up to 15% better efficiency [1] [4].

Useful to conclude, based on all the research done on this thesis, that for the current state of the RES market in Greece, FPV installation alternatives are very difficult to compete with the long-established LBPV technologies, given that they cannot reach the expectations of better performance, with diminished cost. A classic FPV topology with fixed panels installed in a lake, reservoir, or at sea near a coastline, is a costly investment with special-tailored materials lacking in the Greek market, long time-spending bureaucracy, and expertized personnel for mechanical & electrical installations.

*End of this report.*

## References

---

- [1] Z. Golroodbari and W. V. Shark, Simulation of performance differences between offshore and land-based photovoltaic systems., Utrecht: Copernicus Institute, Utrecht University,.
- [2] "https://www.nsenergybusiness.com/features/largest-solar-power-plants/," [Online].
- [3] C.I.A., The world factbook, US, 2017.
- [4] M. Rosa-Clot and M.-G. Tina, Submerged and Floating Photovoltaic Systems, Modelling, Design and Case Studies.
- [5] M. Grech, L. M. Stagno, M. Aquilina, M. Cadamuro and U. Witzke, "Floating photovoltaic installation in Maltese sea," OSES-2016, Malta, 2016.
- [6] N. Martí'n-Chivelet, Photovoltaic potential and land-use estimation methodology, Energy 94, 2016.
- [7] G. Tina and G. Notton, Thermal models for photovoltaic modules in the BIPV applications, Valencia: 25th European Photovoltaic Solar Energy Conference and Exhibition/5th World Conference on Photovoltaic Energy Conversion, 2010.
- [8] C. Z. H. V. L. Jian Dai, K. K. Ang, X. Qian, J. L. H. Wong, S. T. Tan and C. L. Wang, Design and Construction of Floating Modular Photovoltaic System for Water Reservoirs, <https://doi.org/10.1016/j.energy.2019.116549>..
- [9] "pv-mag," 20 3 2020. [Online]. Available: <https://www.pv-magazine.com/2020/03/20/fossil-fuel-giants-bet-on-offshore-pv/>.
- [10] "Offshore-Energy," [Online]. Available: <https://www.offshore-energy.biz/sunseap-installs-one-of-worlds-largest-offshore-floating-solar-farms-in-singapore/>.
- [11] "Swimsol," [Online]. Available: <https://swimsol.com/solar-projects/heavy-duty-roofsolar-power-photovoltaics-maldives-lux-resort/>.
- [12] S. Philipps, "Solar Cell Efficiency Tables, Version 1-48.," in *Progress in Photo voltaics: Research and Applications*, Fraunhofer ISE 2016, 1993-2016.
- [13] K. Trapani and D. L. Millar., "The thin film flexible floating PV (T3F-PV) array: The concept and development of the prototype".
- [14] S. Electric, Electrical Installation Guide, Schneider Electric, 2016.
- [15] J. SJ, P. AB, B. V and B. J, "An analysis of the meteorological variables leading to apparent temperature in australia: present climate, trends, and global warming simulations.," Global Planetary Change.
- [16] P. M. Collaborative, "Sandia Module Temperature Model," [Online]. Available: <https://pvpmmc.sandia.gov/>.

- [17] R. Stewart, "Ocean-Wave Spectra," Wikiwaves-Geophysics, [Online]. Available: [https://wikiwaves.org/Ocean-Wave\\_Spectra](https://wikiwaves.org/Ocean-Wave_Spectra).
- [18] F. Exchange, MathWorks, 2 4 2021. [Online]. Available: <https://www.mathworks.com/matlabcentral/fileexchange/70082-wavemodeling>.
- [19] T. Gurupira and A. J. Rix, PV Simulation Software Comparisons: PVSYST, NREL SAM AND PVLIB, SAUPEC 2017, 2017.
- [20] T. Klucher, Evaluation of models to predict insolation on tilted surfaces., Solar Energy 23 (2), 111-114, 1979.
- [21] Loutzenhiser and e. al., Empirical validation of models to compute solar irradiance on inclined surfaces for building energy simulation., 2007.
- [22] R. Cazzaniga, M. Rosa-Clot, M. Circu and G. Tina, Floating tracking cooling concentrating (FTCC) systems, Austin, TX, USA: 2012 38th IEEE Photovoltaic Specialists Conference, 2012.
- [23] D. King, J. Kratoch, W. Boyson and e. al., Temperature coefficients for PV modules and arrays: measurement methods, difficulties, and results., Conference Record of the Twenty Sixth IEEE Photovoltaic Specialists Conference - 1997, 1997.
- [24] Y. Liu, D. Chen and e. al, Wind Profiles and Wave Spectra for Potential Wind Farms in South China Sea. Part I: Wind Speed Profile Model, MDPI, 2017.

## Table of Figures

---

Figure 1: Potential of FPV installations, from different climate zones, (assume land usage=1%). [3] .....	3
Figure 2: HPDE modules for Photov. Panels support at 500kW FPV Plant in Singapore. ....	8
Figure 3: Specific standing panel base made of PVC, courtesy of Ciel & Terre.....	9
Figure 4: Terra Moretti & Chengiou FPV plant.....	10
Figure 5: Cabling Routing in Huainan FPV Plant, Eastern China.....	10
Figure 6: Swimsol 191kW coastal FPV Plant, South Ari Atoll, Maldives.....	11
Figure 7: Photovoltaic Panel technologies and their highest laboratory efficiencies, graph of Simon Philipps, Fraunhofer ISE 2016.....	13
Figure 8: Transmitted radiation as a function of water depth, courtesy of [4].....	14
Figure 9: Bandgap & cut-off wavelength for various panel technologies. ....	15
Figure 10: Photoelectric efficiency at different solar spectrum, EG & $\lambda$ G. ....	15
Figure 11: Kp coefficient for various panel technologies and number of modules, courtesy of [5].....	16
Figure 12: Circuit Diagram of a ground fault created by a photovoltaic array with TN-S grounding method, Guidance on Proper Residual Current Device Selection for Solar Inverters (white paper), Schneider Electric.	21
Figure 13: Diagram of Protection and Control equipment for a PV plant 20-1000KWp, courtesy of ABB. ....	22
Figure 14: Typical Resistance ( $\Omega$ m) for various types of soil, DEHN 2014, p.121.....	25
Figure 15: Typical electrical DC to AC distribution of a FPV with TN-S grounding system. Upsolar 100kWp FPV park, Singapore. ....	27
Figure 16: Circuit diagram of DC-Grounding method with isolated inverters, courtesy of Fluke.....	28
Figure 17: Location of the Offshore FPV plant in Souda Bay, Crete, Greece (via Google Maps).....	31
Figure 18: Location of the Inshore FPV park in Agia Lake, Crete, Greece (via Google Maps).....	31
Figure 19: Location of the Land-Based PV Park in Agia Lake, Crete, Greece .....	32

Figure 20: Total POA Irradiance Received from Each Case Study PV Model, from simulation results.....	33
Figure 21: Wind Speed Rates Distribution recorded in a Typical Meteorological Year for Inshore FPV (right) and Offshore FPV (left), data source: PVGIS.....	35
Figure 22: Case study selected Inverter Technical Data & Specifications, curtesy of KACO (Left) and PV modules Technical Data (Right), curtesy of HIT.....	40
Figure 23: DNI irradiation received by Land Based PV and Offshore PV. ....	42
Figure 24: POA irradiation received throughout a Typical Month (August). ....	43
Figure 25: Cell temperature throughout a Typical Year for each PV system. ....	44
Figure 26: Basic characteristics and results for each case study, AC Power produced is extracted from our simulation analysis.....	46
Figure 27:Simulation Results of Daily Energy Produced by Each PV System in a TMY.....	47
Figure 28: Simulation Results of Module Temperature Recorded in a TMY. ....	47
Figure 29: Monthly Energy Produced by Each PV Model.....	48
Figure 30: 1 Axis Tracking & Water Veil Cooling Design for FPV Parks, curtesy of [5]. ....	50